

# Photochemical Production and Photolysis of Acrylate in Seawater

Lei Xue and David J. Kieber\*



Cite This: *Environ. Sci. Technol.* 2021, 55, 7135–7144



Read Online

ACCESS |



Metrics & More



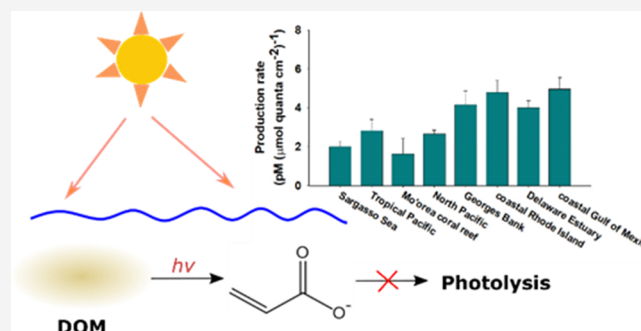
Article Recommendations



Supporting Information

**ABSTRACT:** The marine organosulfur cycle has been studied intensively for over 30 years motivated by the hypothesis that dimethylsulfide (DMS) affects Earth's radiation balance and climate. The main source of DMS is from the enzymatic lysis of dimethylsulfoniopropionate (DMSP), the latter of which is a significant component of carbon, sulfur, and energy fluxes in the oceans. Acrylate is also produced during DMSP lysis, but unlike DMS or DMSP, very little is known about the marine acrylate cycle. Herein, a new source of acrylate was identified in seawater as a product formed from the photolysis of dissolved organic matter (DOM). Photochemical production rates varied from 1.6 to 5.0 pM ( $\mu\text{mol quanta cm}^{-2}\text{s}^{-1}$ ), based on photon exposures determined from nitrite actinometry. A positive correlation ( $r = 0.87$ ) was observed between acrylate photoproduction and the seawater absorption coefficient at 330 nm. Acrylate photoproduction was initiated by UV radiation, with UV-B and UV-A contributing approximately 32 and 68% to the total production, respectively. Acrylate did not photolyze in high-purity water or seawater at concentrations less than 100 nM. These findings improve our understanding of the role that sunlight plays in the marine acrylate cycle, a reactive form of DOM that significantly affects the carbon cycle and ecology of the upper ocean.

**KEYWORDS:** dimethylsulfide, dimethylsulfoniopropionate, dmsp, dms, actinometry, phytoplankton, acrylic acid



## INTRODUCTION

Acrylate and dimethylsulfide (DMS) are produced in the oceans from the enzymatic cleavage of dimethylsulfoniopropionate (DMSP), a key organosulfur compound produced by many important marine phytoplankton,<sup>1,2</sup> corals,<sup>3</sup> and several marine bacteria.<sup>4,5</sup> DMS and DMSP have been studied extensively due to their importance in upper ocean biogeochemistry and climate regulation, but studies investigating acrylate cycling in seawater are rare despite its expected prevalence in the ocean, given the ubiquity of DMSP and DMSP lyase enzymes and the importance of DMSP in marine phytoplankton. Acrylate concentrations and fluxes should be particularly high during blooms of phytoplankton species containing high levels of DMSP and DMSP lyase enzymes, as suggested by laboratory culture studies (e.g., *Phaeocystis antarctica*)<sup>6</sup> and during *Phaeocystis* sp. blooms in Antarctic coastal waters where acrylate concentrations can approach micromolar levels.<sup>7,8</sup>

Acrylate is proposed to serve several important physiological functions in marine phytoplankton. Acrylate, together with DMSP, constitute an antioxidant system due to their high cellular concentrations and efficiency at scavenging reactive oxygen species (ROS) in several marine algae.<sup>6,9</sup> Cellular acrylate production and its subsequent removal may also function as part of a carbon overflow mechanism.<sup>10</sup> When its concentration is sufficiently high, acrylate can serve as an activated defense system against bacteria,<sup>11,12</sup> grazing,<sup>13,14</sup> and

viruses.<sup>15</sup> However, these inhibitory functions may not be important when acrylate is present in seawater at nM concentrations or when acrylate is sorbed in a mucus matrix such as in *Phaeocystis globosa*<sup>16</sup> and not available to the surrounding planktonic community. Instead, acrylate may play a role in shaping the mucus in colonial marine phytoplankton.<sup>16</sup>

Known sources of acrylate in seawater include (1) its abiotic production from the  $\beta$ -elimination reaction between DMSP and the hydroxide anion, albeit this source is insignificant because the reaction is very slow at the alkaline pH of seawater (ca. 8.0) with a half-life of about 8 years at 10 °C;<sup>17</sup> and (2) the enzymatic cleavage of DMSP. Rates for acrylate production from enzymatic DMSP cleavage have not been reported but can be estimated based on DMS production rates. DMS is produced in seawater from the cleavage of DMSP by lyase, with production rates that vary from <0.1 to 7.7 nM day<sup>-1</sup> in a broad range of marine environments.<sup>18–26</sup> Acrylate should be produced at similar rates since DMS and acrylate are formed in

Received: January 18, 2021

Revised: April 8, 2021

Accepted: April 21, 2021

Published: May 6, 2021

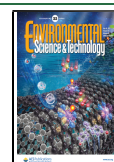


Table 1. Photochemical Production of Acrylate in 0.2  $\mu\text{m}$ -Filtered Seawater Samples Exposed to Sunlight<sup>a</sup>

sampling location	lat. (°N)	long. (°W)	salinity (ppt)	$a_{330}$ (m <sup>-1</sup> )	acrylate (nM)	photon exposure ( $\mu\text{mol quanta cm}^{-2}$ )		production rate (pM ( $\mu\text{mol quanta cm}^{-2}$ ) <sup>-1</sup> )
						311–333 nm <sup>b</sup>	330–380 nm <sup>c</sup>	
North Pacific	55.85	153.04	36.1	0.37	0.47 (0.08)	27.7 (0.9)	176.2 (5.7)	2.7 (0.5)
GOM open ocean <sup>d</sup>	28.47	92.23	36.0	0.19	0.48 (0.18)	32.5 (2.0)	206.9 (6.6)	2.3 (0.6)
GOM coastal	28.96	90.79	29.9	1.05	1.16 (0.13)	28.7 (1.1)	231.8 (7.2)	5.0 (0.6)
coastal Rhode Island	41.02	71.18	32.6	0.66	0.79 (0.16)	25.3 (1.3)	161.4 (4.4)	4.8 (0.6)
Georges Bank	41.40	67.48	32.5	0.56	0.88 (0.15)	32.3 (1.4)	208.8 (8.6)	4.2 (0.7)
Delaware Estuary	38.78	74.94	31.5	0.92	0.95 (0.07)	31.3 (1.2)	236.5 (10.5)	4.0 (0.4)
Pacific Ocean	-17.46	149.84	36.5	0.07	1.34 (0.52)	76.3 (3.5)	580.7 (21.5)	2.3 (0.6)
Mo'orea coral reef	-17.48	149.84	36.5	0.14	0.66 (0.33)	54.3 (2.6)	405.5 (13.5)	1.6 (0.4)
Sargasso Sea	35.00	69.99	36.4	0.06	0.47 (0.08)	57.6 (1.8)	236.8 (5.2)	2.0 (0.3)

<sup>a</sup> $a_{330}$  is the initial absorption coefficient at 330 nm. The concentration of acrylate produced during a photochemical experiment and reported in this table is the difference in the concentration in the light-exposed sample minus the concentration in the dark control. The production rate was calculated by dividing the acrylate concentration by the photon exposure determined by nitrite actinometry. The standard deviation is reported in parentheses. Refer to the map in Figure S1 for the location of the sampling stations. Errors for  $a_{330}$  were less than 2% and for clarity are not shown in the table. <sup>b</sup>Nitrate actinometry. <sup>c</sup>Nitrite actinometry. <sup>d</sup>GOM denotes the Gulf of Mexico.

equimolar quantities from the biological cleavage of DMSP by lyase.

Acrylate is removed from seawater through its bacterial consumption for growth as a carbon and energy source, as suggested by several field and laboratory culture studies.<sup>16,27–29</sup> The biological consumption of acrylate by heterotrophs in Gulf of Mexico seawater followed first-order kinetics, with a consumption rate constant ( $k_{\text{bio}}$ ) ranging from 0.045 to 1.2 day<sup>-1</sup>; a large fraction of the acrylate consumed by the heterotrophic community was assimilated (22–60%) or respired to CO<sub>2</sub> (16–40%).<sup>30</sup>

A second proposed removal pathway for acrylate is through its photolysis. Bajt et al.<sup>31</sup> and Wu et al.<sup>32</sup> observed that  $\mu\text{M}$  concentrations of acrylate photolyzed in seawater and high-purity laboratory water when solutions were exposed to artificial solar radiation or sunlight. In both studies, a matrix dependence was observed for photolysis suggesting the involvement of photosensitized reactions. Additionally, the photolysis rate constant decreased by an order of magnitude, from 3 to 0.2 h<sup>-1</sup> and from 0.06 to 0.005 h<sup>-1</sup>, with increasing initial acrylate concentration from 7 to 280  $\mu\text{M}$ <sup>31</sup> and from 0.5 to 10  $\mu\text{M}$ ,<sup>32</sup> respectively, when using artificial radiation from a filtered mercury or xenon lamp as the light source. Acrylate concentrations used in these photolysis experiments were 2 to 4 orders of magnitude greater than those under most oceanic settings (e.g., 1–5 nM; 0.8–2.1 nM).<sup>30,33</sup> Therefore, extrapolation of these results<sup>31,32</sup> to ambient concentrations may not be warranted as the mechanism for photolysis at nM concentrations may be quite different from that observed at micromolar levels.

In the present study, we identified a new source of acrylate in seawater from the photolysis of dissolved organic matter in 0.2  $\mu\text{m}$ -filtered seawater exposed to solar radiation and furthermore showed that acrylate does not photolyze in seawater at nM concentrations. These results provide new, fundamental information on the role of sunlight in the cycling of acrylate in the upper ocean.

## MATERIALS AND METHODS

**Chemicals and Glassware.** Sodium acrylate (97%), sodium acetate (99%, ACS reagent grade), DMSP hydrochloride (96%), and sodium nitrate (99.995%) were

purchased from Sigma-Aldrich. *o*-Thiosalicylic acid (TSA, 98%) was obtained from Acros Chemicals. Sodium nitrite (>99%) was purchased from Fluka Chemical. Sodium hydroxide pellets (97%, ACS grade) were purchased from Alfa Aesar. Salicylic acid (99.5%), benzoic acid, and sodium bicarbonate (reagent grade) were purchased from J. T. Baker. Benzoic acid was recrystallized three times using purified laboratory water. Ultrex-grade hydrochloric acid (12 M, BDH) and glacial acetic acid (17.4 M) were from EMD. HPLC-grade acetonitrile (ACN) and methanol (MeOH) were obtained from J. T. Baker. High-purity laboratory water (>18.2 M $\Omega$  cm, hereafter referred as Milli-Q water) used throughout this study was obtained from a Milli Q gradient A10 ultrapure water system (EMD Millipore, Billerica, MA).

All borosilicate glassware was rinsed with Milli-Q water and mu ed at 550 °C for 8 h prior to use. Qorpak bottles were further rinsed several times with 0.2  $\mu\text{m}$ -filtered seawater just prior to sample collection. Thermoset screw caps with Teflon-faced silicone inserts were used to tightly seal Qorpak glassware before and after seawater sampling. Quartz tubes with Teflon end fittings<sup>34</sup> used in the photochemical experiments were rinsed copiously with Milli-Q water.

**Acrylate Standards and Quantification.** Acrylate standards were prepared by adding 1 mL of a 10 M NaOH solution to 10 mL of a 5 mM DMSP standard in a 30 mL borosilicate serum vial that was crimp capped with an aluminum seal containing a Teflon-faced butyl rubber stopper. The basified standard reacted overnight at room temperature to quantitatively convert DMSP to equimolar quantities of acrylate and DMS.<sup>17</sup> The reacted solution was bubbled with ultrapure He (99.9995%) to remove DMS followed by neutralization using 12 M Ultrex HCl. The purity of the DMSP standard was determined using a total carbon analyzer calibrated with potassium hydrogen phthalate (ACS acidimetric standard, 99.95–100.05%, Sigma Aldrich).

Acrylic acid or acrylate salts were not used to make standards in our study for two reasons. First, all commercially available grades of acrylic acid contain a stabilizer (e.g., 4-methoxyphenol) that would interfere with photolysis experiments, and second, acrylate salts (e.g., sodium acrylate) degrade after several weeks when stored in the dark.<sup>35</sup>

All samples were analyzed for acrylate using a precolumn derivatization HPLC method.<sup>30</sup> Briefly, the derivatization procedure consisted of adding 300  $\mu\text{L}$  of TSA reagent (20 mM TSA in MeOH) to 3 mL of Milli-Q water or seawater sample in a Qorpak borosilicate vial at pH 4.0. Tightly capped vials were placed in a 90 °C water bath for 6 h. To inject a derivatized sample, it was filtered through a 0.2  $\mu\text{m}$  Nylon syringe filter directly into the HPLC injection port. The acrylate derivative was quantified by reversed-phase HPLC with UV absorption detection at 257 nm. The limit of detection was 0.2 nM for a 1.0 mL injection of the derivatized sample with a signal-to-noise ratio of 2.

**Seawater Sample Collection.** Water samples were collected from several sites in the Pacific Ocean, the Atlantic Ocean, and the Gulf of Mexico (Table 1, Figure S1). Seawater samples were collected at 5 m in Niskin bottles, except for the Mo'orea samples that were collected using an all-polypropylene bucket using an attached polypropylene rope. Once onboard, the seawater was poured from the bucket into an opaque 10 L high-density polyethylene (HDPE) bottle leaving no headspace. Seawater samples were gravity filtered directly from the Niskin bottles or 10 L HDPE bottles with silicone tubing through precleaned<sup>36</sup> 0.2  $\mu\text{m}$  pore size POLYCAP 75 AS Nylon filters into 4 L Qorpak glass bottles (Whatman).

Filtered samples were stored in the dark at room temperature until they were transported to Syracuse, NY, after which they were stored in the dark at 4 °C. Samples collected in Mo'orea, French Polynesia, were used the same day in photochemical experiments at the Gump Research Station.

**Chemical Actinometry.** Except when noted, nitrate and nitrite actinometers<sup>37–39</sup> were used to quantify the photon exposure from 311 to 333 nm and 330 to 380 nm, respectively. Nitrate and nitrite actinometer solutions were prepared separately and consisted of either 10 mM sodium nitrate or 1 mM sodium nitrite in a 1 mM benzoic acid solution buffered to pH 7.2 with 2.5 mM sodium bicarbonate. The nitrate and nitrite actinometer solutions were placed in separate borosilicate vials. These vials reduced the nitrate-based photon exposure by 20% compared to quartz but had no effect on the nitrite-actinometer photon exposure.<sup>39</sup> Therefore, a 20% correction was applied to the nitrate actinometry data to scale the photon dose to that of the irradiated seawater solutions in the quartz vessels. Vials containing the nitrite actinometer were wrapped in a Mylar D film to attenuate solar radiation <330 nm and minimize the overlap of the response bandwidths of the two actinometers.<sup>38</sup> All borosilicate vials containing the actinometer solutions were enclosed in neutral density screening, and a screening factor of 0.31 was applied to calculate photon exposures.

**Sunlight-Exposure Experiments.** 0.2  $\mu\text{m}$ -filtered seawater was gently pulled from a 4 L Qorpak glass bottle into eight precleaned, 90 mL Teflon-sealed quartz tubes with no headspace;<sup>34</sup> prior to filling, each quartz tube was rinsed several times with the filtered seawater. Four quartz tubes were exposed to sunlight, and four quartz tubes were wrapped with aluminum foil as dark controls. Quartz tubes and triplicate nitrate and nitrite actinometry samples<sup>39</sup> were submerged in a 2 cm-deep circulating water bath at  $22 \pm 1$  °C (or 28–30 °C at the Gump Research Station) and exposed to sunlight for 8 to 30 h over 1 to 3 days, depending on the sample (Table S1); solar irradiation experiments were conducted in April at the Gump Research Station or sometime between August and

October in Syracuse, NY (Table S1). At the end of an experiment, an aliquot of each quartz tube was transferred into a precleaned 20 mL scintillation vial and frozen at  $-20$  °C until further analysis.

During the field campaign in Mo'orea, photochemical experiments were conducted using freshly collected, 0.2  $\mu\text{m}$ -filtered seawater from the coral reef and open ocean stations. The experimental setup was the same as used for stored samples, except for the differences noted above (e.g., warmer water bath). Additionally, at the end of each Mo'orea sunlight-exposure experiment, a 15 mL aliquot of each sample was transferred to a 20 mL borosilicate scintillation vial and acidified with 150  $\mu\text{L}$  of 12 M HCl and stored at room temperature in the dark<sup>40</sup> until analysis in Syracuse, NY. All actinometer solutions were stored frozen until analysis using batch fluorescence spectroscopy at the Gump Research Station.<sup>39</sup>

**Wavelength Dependence.** An experiment was performed to determine the contribution of UV-B (290–320 nm) and UV-A (320–400 nm) to the photochemical production of acrylate in 0.2  $\mu\text{m}$ -filtered seawater collected from Georges Bank (Figure S1). Filtered seawater was transferred to three quartz tubes with no Mylar, three quartz tubes each wrapped with Mylar D film, and three quartz tubes wrapped in several layers of aluminum foil. All samples were exposed to sunlight for several days, equivalent to a total solar exposure time of approximately 20 h. Acrylate concentrations in the sunlight-exposed quartz tubes were compared to concentrations in the quartz tubes wrapped with Mylar D film and the dark controls. The in Mylar D film had 0% transmission at 313 nm and 50% transmission at 320 nm, approximating a UV-B filter.<sup>41</sup>

**Time-Series Solar Simulator Experiments.** A 300 W xenon lamp (Atlas Specialty Lighting) was used as the light source to study the photochemical production and photolysis of acrylate in seawater in the laboratory. To simulate the spectral output of sunlight, the lamp output was filtered through Milli-Q water to remove IR radiation followed by a Pyrex plate with 3.3% transmission at 290 nm; the resultant spectral output is shown in Figure S2. The lamp intensity was adjusted to approximately 7.5 suns to study the time-course for acrylate photoproduction or photolysis. For photochemical production experiments, 0.2  $\mu\text{m}$ -filtered, air-saturated seawater was exposed to the solar simulator in a 70 mL round-bottom quartz flask fitted with a 24/40 solid Teflon stopper and Teflon-coated magnetic stirrer. For photolysis experiments, an aqueous acrylate standard, prepared from the hydrolysis of DMSP, was added to Milli-Q water or seawater to a final concentration of 20 or 100 nM. The temperature was maintained at  $21 \pm 1$  °C. Subsamples were taken at several time points to determine the concentration of acrylate and chromophoric dissolved organic matter (CDOM) absorbance. The photon exposure was determined using nitrite actinometry in a separate 70 mL round-bottom quartz flask using the same starting volume used for the seawater samples and taking the same 6 mL subsample per time point.

**Seawater Absorbance.** The absorbance of 0.2  $\mu\text{m}$ -filtered seawater was determined from 240 to 600 nm using a SD-2000 fiber optic spectrophotometer (Ocean Optics, Inc.) coupled to a 101 cm long liquid waveguide capillary cell (World Precision Instruments). The capillary waveguide was cleaned by flushing with alternate rinses of Milli-Q water and MeOH. The capillary-cell path length was determined according to Cartisano et al.<sup>42</sup> A Rainin Rabbit-Plus peristaltic pump was

used to gently pull seawater, Milli-Q water, or MeOH through the cell. CDOM absorption coefficients ( $a$ ) were calculated from the corrected sample absorbance ( $A$ ) and capillary-cell path length ( $l$ ) where  $a = 2.303A/l$ . Milli-Q water was used as the reference solution for all absorbance measurements. All sample absorbances were corrected for offsets by adjusting  $A$  between 630 to 640 nm to zero prior to conversion to  $a$ .

**Statistical Analyses.** All statistical analyses were carried out using Sigmaplot 11.0 with the SigmaStat software package (Systat Software). Normality was tested for all data sets using the Shapiro–Wilk test. An  $\alpha$  level of 0.05 was used for all statistics.

## RESULTS AND DISCUSSION

**Acrylate Photochemical Production.** Acrylate production was observed in all sunlight-exposed samples (Figure 1).

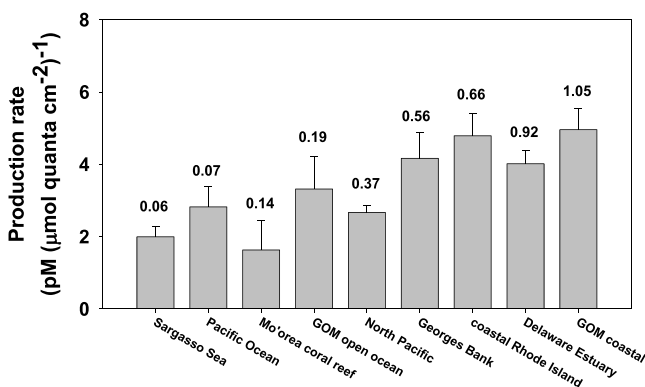


**Figure 1.** Photoproduction rate of acrylate in 0.2  $\mu\text{m}$ -filtered seawater collected from several oceanic waters. Production rates were calculated by dividing the net (light – dark) acrylate concentration produced in the photochemical experiments by the photon exposure between 330 and 380 nm determined by nitrite actinometry (Table 1). The value above each error bar is the absorption coefficient at 330 nm ( $\text{m}^{-1}$ ). Error bars denote the standard deviation of measurements from multiple quartz tubes ( $n = 4$ ). GOM denotes the Gulf of Mexico. Station locations are given in Table 1 and Figure S1.

By contrast, no accumulation or loss of acrylate was seen in the dark controls, indicating that the production of acrylate was due to a sunlight-dependent process. To directly compare results across different experiments and accurately account for seasonal differences and cloud cover effects on photochemical production rates of acrylate,<sup>39</sup> production rates were expressed as a function of the UV photon exposure (instead of exposure time) between 330 and 380 nm as determined by nitrite actinometry (Table 1). Photon-based rates increased linearly with increasing  $a_{330}$  ( $r = 0.87$ , Figure 2), and the average production rate was nearly twice as fast in samples with  $a_{330} > 0.5 \text{ m}^{-1}$  ( $4.5 \pm 1.2 \text{ pM } (\mu\text{mol quanta cm}^{-2})^{-1}$ ,  $n = 4$ ) compared to samples with  $a_{330} < 0.4 \text{ m}^{-1}$  ( $2.3 \pm 1.0 \text{ pM } (\mu\text{mol quanta cm}^{-2})^{-1}$ ,  $n = 5$ ). We selected the absorption coefficient at 330 nm because acrylate photoproduction in seawater peaks at 330 nm.<sup>35</sup> A similar trend of increasing photochemical rates with increasing sample absorbance has been previously observed for several compounds in seawater including aldehydes and ketones<sup>43,44</sup> and carbon monoxide.<sup>45</sup>

For the sunlight-exposure experiments, we saw some CDOM photobleaching (<20% at all wavelengths and mostly <10% at <380 nm). This degree of CDOM photobleaching did not affect photochemical production rates for acrylate in

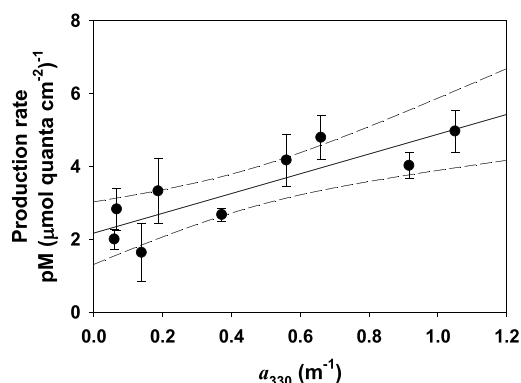


**Figure 2.** Nitrite-based (330–380 nm) photochemical production rate of acrylate in the samples depicted in Figure 1 plotted against the initial absorption coefficient at 330 nm ( $a_{330}$ ). The vertical error bars denote the standard deviation of replicate samples ( $n = 4$ ). The slope and  $y$ -intercept ( $\pm$ std. error) for the linear regression line ( $r = 0.87$ ) are  $2.7 \pm 0.6 \text{ pM m } (\mu\text{mol quanta cm}^{-2})^{-1}$  and  $2.2 \pm 0.4 \text{ pM } (\mu\text{mol quanta cm}^{-2})^{-1}$ , respectively. The dashed lines denote the 95% confidence interval for the best-fit line.

seawater samples exposed to sunlight. This is a reasonable assumption because, for this degree of photobleaching, the accumulation of acrylate was a linear function of the photon exposure (Figure 3), and therefore, the photochemical production rate of acrylate was constant. It was only when UV photon exposures were greater than  $600 \mu\text{mol quanta cm}^{-2}$  between 330–380 nm that accumulation rates decreased. The photon exposure in our sunlight-exposure experiments ranged between 161–581  $\mu\text{mol quanta cm}^{-2}$ , with all except one sample exposed to less than  $400 \mu\text{mol quanta cm}^{-2}$  (Table S1). We have previously shown for carbonyl compounds<sup>46</sup> that photobleaching was only an issue for extended photon exposures when the quantum yields for carbonyl photoproduction decreased (i.e., reciprocity was no longer obeyed). The main uncertainties in our results, and indeed that for anyone who studies photoprocesses in natural waters, are the unknown photobleaching history of samples used in the photochemical experiments and whether CDOM absorption can be used as a proxy to follow/predict the rate of a photochemical reaction in seawater.

Since photochemical production rates of acrylate varied as a function of sample absorbance (Figure 2), it is reasonable to conclude that the photochemical production of acrylate occurred through a primary process or a photosensitized pathway involving CDOM. However, the  $y$ -intercept of the regression line ( $2.2 \pm 0.4 \text{ pM } (\mu\text{mol quanta cm}^{-2})^{-1}$ ) was statistically different from zero at the 95% confidence interval ( $p < 0.001$ ). A linear relationship was also observed when photon-exposure based rates were plotted as a function of the absorption coefficient at  $a_{290}$  or  $a_{390}$  (Figure S3), and although the slopes were different, the  $y$ -intercepts ( $2.0$  and  $2.1 \text{ pM } (\mu\text{mol quanta cm}^{-2})^{-1}$ , respectively) were similar and significantly greater than zero. This nonzero  $y$ -intercept was independent of the UV absorption coefficient used for this plot. This indicates that there is a component of DOM that is involved in acrylate photoproduction in light-exposed samples that does not vary with changes in CDOM absorption. Specifically, (1) there may be nonabsorbing components of DOM that result in acrylate photoproduction via photosensitized reactions involving CDOM either through type I or II photosensitized reactions or (2) there are one or more

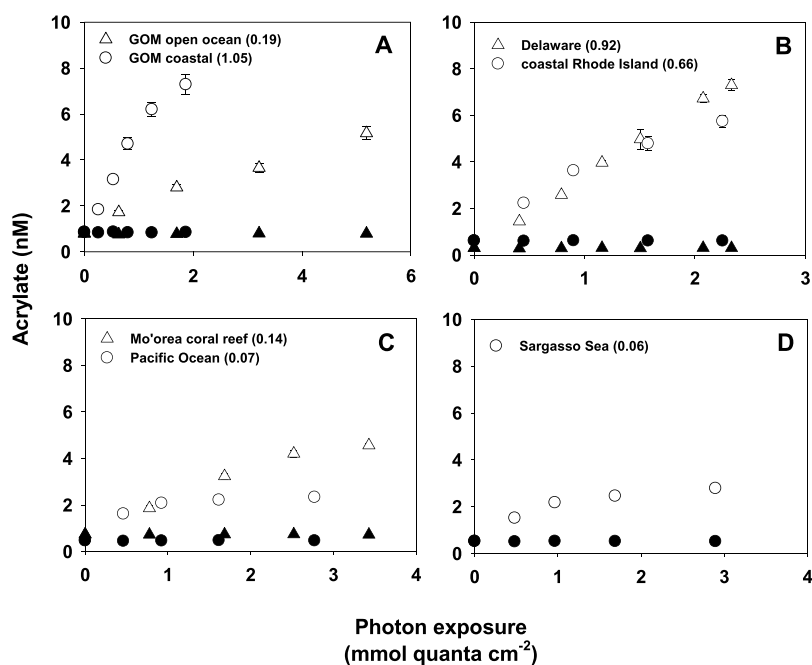


**Figure 3.** Acrylate concentrations plotted against the nitrite-based photon exposure in  $0.2 \mu\text{m}$ -filtered samples from the (A) Gulf of Mexico (GOM), (B) coastal Atlantic Ocean, (C) Mo'orea coral reef and Pacific Ocean, and (D) Sargasso Sea. The values in parentheses in the panel legends are the CDOM absorption coefficients at 330 nm ( $\text{m}^{-1}$ ). Filled symbols in each panel depict dark controls. Vertical error bars denote the standard deviation of replicate samples ( $n = 3$ ); the error for most samples is smaller than the symbol.

minor absorbing CDOM components present at very low concentrations (e.g., nM) with high quantum yields for acrylate photoproduction that were not captured by variations in the total CDOM absorption. Although no definitive conclusion can be drawn regarding this “background” photoproduction, it is nonetheless significant because it accounts for a considerable proportion of acrylate photoproduction in seawater. This finding also indicates that there are at least two components to acrylate photoproduction. Further investigation is warranted to determine if this is a common feature for other photoprocesses in seawater and freshwater and to better understand the process(es) that give rise to this nonzero  $y$ -intercept for acrylate photoproduction.

Acrylate photochemical production rates were compared to other similar low-molecular-weight organic photoproducts produced in seawater. For this comparison, average hourly clear-sky production rates were calculated for acrylate (Section S1). Although not directly comparable to published rates because of seasonal differences and differences in how hourly rates are reported, this comparison is nonetheless useful to qualitatively compare rates to highlight general trends and large differences. Average hourly production rates of acrylate ranged from  $0.034$  to  $0.14 \text{ nM h}^{-1}$ . Although orders of magnitude slower than CO or  $\text{CO}_2$  photoproduction rates,<sup>47,48</sup> acrylate photoproduction rates are comparable to rates reported for several low-molecular-weight compounds including glyoxal and methylglyoxal in Atlantic Ocean surface waters during September–October ( $0.06$ – $0.2$  and  $0.02$ – $0.07 \text{ nM h}^{-1}$ );<sup>49</sup> rates are at the lower end of the range of noontime production rates reported for several other low-molecular-weight compounds including glyoxylic acid, pyruvic acid, and glyoxal in Sargasso Sea surface waters ( $0.4 \pm 0.2$ ,  $0.2 \pm 0.1$ , and  $0.4 \pm 0.2 \text{ nM h}^{-1}$ ).<sup>47</sup> Acrylate photoproduction rates are much lower, by 1 to 2 orders of magnitude, than the noontime rates for the two simplest aldehydes, formaldehyde ( $0.5$ – $11.4$

$\text{nM h}^{-1}$ ) and acetaldehyde ( $0.2$ – $9.0 \text{ nM h}^{-1}$ ), in waters from the Sargasso Sea, Biscayne Bay, Hatched Bay, Hiroshima Bay, and northwest Atlantic Ocean determined in the summer.<sup>43,47,49–52</sup>

The photochemical production of acrylate is an important component of the marine acrylate cycle in surface waters. Between  $0.34$  and  $1.44 \text{ nM}$  acrylate is produced photochemically on a daily basis in the seawater samples examined in this study. This daily production is comparable to the concentration of dissolved acrylate observed in these samples, which ranged from  $0.4$  to  $1.5 \text{ nM}$ . In the Gulf of Mexico, daily photochemical production rates of acrylate determined here were  $0.48 \text{ nM day}^{-1}$  in open-ocean waters and  $1.16 \text{ nM day}^{-1}$  in coastal waters. Corresponding biological consumption rates in these same water samples<sup>30</sup> were, on average,  $0.24$  and  $0.96 \text{ nM day}^{-1}$ , respectively. Rates of production and removal were comparable for these Gulf of Mexico samples, suggesting that photochemical production of acrylate is fast enough to support the role of acrylate as a substrate for energy and growth in surface seawater by that fraction of the heterotrophic community that consumed acrylate.

**Time-Series Experiments.** Filtered seawater samples were exposed to radiation from the solar simulator to determine the time-course change in the concentration of acrylate as a function of the nitrite-based photon exposure. The higher light intensities provided by the solar simulator were necessary to have the sensitivity to see concentration differences between time points in the time course for production with increasing photon exposure; this experiment was not possible using sunlight directly as production rates were too slow. Samples irradiated for 4 h in the solar simulator had a photon exposure of  $1 \text{ mmol quanta cm}^{-2}$  between 330 and 380 nm, which is equal to approximately 4 days of solar irradiation (at 9 h per day, 8:00–17:00 local time) under cloudless, summertime conditions in Syracuse, NY ( $43.0^\circ \text{N}$ ,  $76.1^\circ \text{W}$ ).

The concentration of acrylate increased linearly in all seawater samples with increasing photon exposure in the solar simulator, with the higher light-absorbing waters exhibiting a greater potential for the photochemical production of acrylate (Figure 3). For example, approximately 7 nM acrylate was produced in the coastal Gulf of Mexico sample compared to 1.4 nM produced in the Gulf of Mexico open-ocean water sample after 10 h of exposure to the solar simulator. However, acrylate production did not increase linearly indefinitely with increasing photon exposure, but rather, it eventually slowed down or leveled off with no further change. Since acrylate does not photolyze in seawater at ambient concentrations (*vide infra*), the lack of acrylate production observed with prolonged photon exposure was not due to a steady state balance between production and photolysis. Instead, the observation that acrylate did not change over time at long photon exposures was due to (1) a change in the mechanism involving reactions that may compete with or quench reactions that produce acrylate or (2) the complete removal of the precursor(s) or CDOM photosensitizers in seawater that led to the photochemical production of acrylate. The potential for precursor or photosensitizer removal was likely given that there was a significant loss in CDOM absorbance in seawater samples exposed to the solar simulator for an extended period of time (Figure S4; e.g., up to 65% loss at 330 nm in some samples).

To assess whether the solar simulator results can be extrapolated to (and are comparable to) results obtained from sunlight-exposure experiments, initial production rates determined with the solar simulator were plotted against corresponding rates determined using sunlight (Figure S5). For this comparison, all rates were calculated based on the photon exposure determined by nitrite actinometry. Correlation analysis ( $r = 0.94$ ) yielded a slope ( $\pm$ std. error) of  $0.94 \pm 0.09$  that was not significantly different from a slope of 1.0 based on a two-tailed  $t$  test ( $p < 0.0001$ ). Based on this finding, it is reasonable to conclude that the higher light intensities used in the solar simulator experiments (7.5 suns) did not affect production rates in a nonlinear fashion, and therefore, results from solar-simulator experiments are representative of sunlight-based rates when photon exposures are scaled to ambient light conditions.

**Spectral Dependence for Photoproduction.** The average production ( $\pm$ std. dev) of acrylate in 0.2  $\mu\text{m}$ -filtered Georges Bank seawater exposed to full spectrum sunlight in quartz tubes for 3 days was  $3.0 \pm 0.2$  nM based on the difference in the acrylate concentration between the light and dark controls (Figure 4). The difference in the acrylate concentration between the sunlight-exposed quartz tubes and the Mylar-wrapped quartz tubes was  $1.0 \pm 0.2$  nM. This difference yielded the acrylate production at wavelengths less than 313 nm, approximately corresponding to the UV-B. A smaller difference was observed between the acrylate concentration in the Mylar D film wrapped quartz tube samples exposed to sunlight and the dark control ( $2.1 \pm 0.1$  nM), representing acrylate production greater than 313 nm. It is assumed that there is negligible acrylate production in seawater stemming from visible solar radiation. This is a reasonable assumption based on wavelength-dependent quantum yield results that show that acrylate photoproduction only occurs at wavelengths less than 390 nm in seawater samples spanning coastal to blue waters in the ocean.<sup>35</sup> When only considering solar UV radiation, the relative contributions of UV radiation less than and greater than 313 nm were 32 and

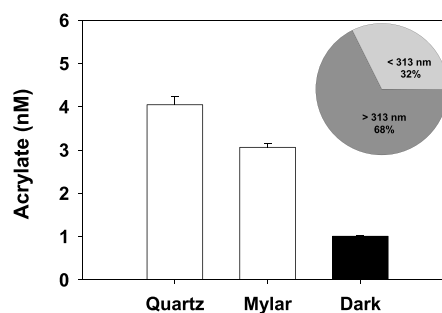


**Figure 4.** Acrylate concentration measured in 0.2  $\mu\text{m}$ -filtered Georges Bank seawater exposed to sunlight for 3 days in quartz tubes (Quartz), Mylar-wrapped quartz tubes (Mylar), and aluminum foil-wrapped quartz tubes (Dark controls). The pie graph shown in the inset depicts the relative contribution of  $< 313$  nm solar radiation (i.e., the difference between the production in the quartz tube and Mylar-wrapped quartz tube) and  $> 313$  nm solar radiation (i.e., the difference between the production in the Mylar-wrapped quartz tube and the dark control) to the total photochemical production of acrylate. Error bars denote the standard deviation of multiple tubes for each spectral treatment ( $n = 3$ ).

68%, respectively, suggesting that UV-A played a proportionately greater role than UV-B in the photochemical production of acrylate in seawater.

The importance of UV-A in the photochemical production of acrylate in seawater is in line with that determined for the photochemical production of CO and CO<sub>2</sub>,<sup>48</sup> hydrogen peroxide,<sup>41</sup> carbonyl compounds (formaldehyde,<sup>44</sup> acetaldehyde, glyoxal, and methylglyoxal<sup>53</sup>), and the photolysis of DMS<sup>36</sup> and domoic acid.<sup>54</sup> Nearly all compounds studied to date are produced or photolyzed in seawater primarily from UV-A solar radiation. The importance of UV-B by comparison is relatively small (ca.  $< 35\%$ ), especially when considering depth-integrated rates and the faster depth-dependent attenuation of UV-B relative to UV-A in the water column. Nonetheless, a few studies have shown that photochemistry is controlled by UV-B radiation in seawater; UV-B played a major role in the photochemical production of formaldehyde in Biscayne Bay<sup>43</sup> and Southern California coastal seawater.<sup>44</sup> In Antarctic waters, the photochemical production of hydrogen peroxide in an open-ocean station in the Weddell-Scotia Seas and a coastal station in Paradise Harbor had important contributions from both UV-B and UV-A but with proportionately larger contributions from UV-A.<sup>55</sup> However, in a coastal station along the Antarctic Peninsula, Crystal Sound, the photochemical production of hydrogen peroxide was primarily due to UV-B radiation.<sup>55</sup> There is no fundamental reason to expect that spectral dependencies will be the same or similar for a given compound or among different compounds. What can be said, however, is that when differences are noted as seen for formaldehyde or hydrogen peroxide, they are likely due to differences in the types and concentrations of precursors present in the water samples.

**Acrylate Photolysis.** Acrylate may undergo primary photolysis in seawater since it weakly absorbs solar radiation 290 nm (Figure 5A), corresponding to an n-to- $\pi^*$  transition.<sup>56</sup> To estimate the maximum photolysis rate that may be expected in surface seawater, we assumed the quantum yield for primary photolysis was unity. With this assumption, the maximum rate constant ( $k_{\text{max}}$ ) for acrylate primary photolysis<sup>57</sup> is

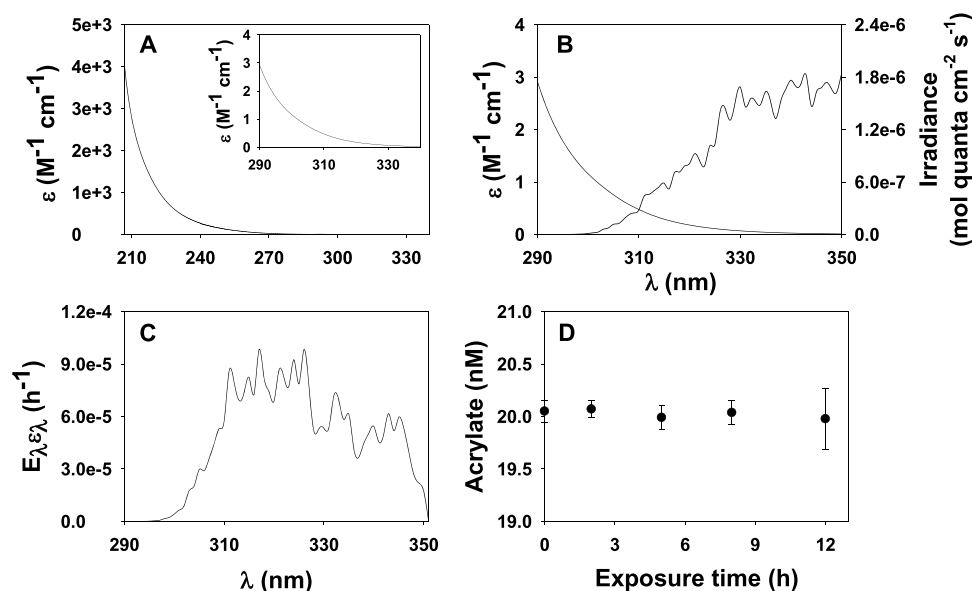


**Figure 5.** (A) Acrylate molar absorptivity ( $\epsilon$ ) at pH 7.2 in 5.0 mM bicarbonate buffer in the spectral range between 207 and 350 nm. (B)  $\epsilon$  and the solar irradiance ( $E$ ) plotted as a function of wavelength. (C) The product  $E\lambda$  between 290 and 350 nm. This product depicts the bandwidth wherein primary photolysis of acrylate may occur at the sea surface. The  $E$  used for this calculation is the noontime solar radiation spectrum on a clear-sky day on September 12, 2011, in the Gulf of Mexico (28.5 °N, 90.5 °W). (D) Time-course acrylate concentration in a 20.1 nM acrylate standard in Milli-Q water at circumneutral pH exposed to radiation from the solar simulator for 12 h; the corresponding nitrite-based photon exposure was 3.5 mmol quanta  $\text{cm}^{-2}$ . Vertical error bars denote the standard deviation for replicate treatments ( $n = 3$ ).

$$k_{\max} = \int_{290}^{350} \epsilon_{\lambda} E_{\lambda} d\lambda \quad (1)$$

where  $\epsilon$  is the wavelength-dependent molar absorptivity of acrylate at pH 8.2 ( $\text{L mol}^{-1} \text{cm}^{-1}$ ) and  $E$  is the wavelength-dependent noontime, clear-sky solar irradiance ( $\text{mol quanta m}^{-2} \text{s}^{-1}$ ). To determine  $k_{\max}$ , the clear-sky, noontime solar irradiance in the Gulf of Mexico was calculated using the SMARTS version 2.9.5 model (see Section S1 for details); the resultant wavelength-dependent irradiance is depicted in Figure 5B. The wavelength-dependent product of  $\epsilon$  and  $E$  (Figure 5C) was integrated between 290 and 350 nm to yield  $k_{\max}$ .

The calculated noontime  $k_{\max}$  was  $0.002 \text{ h}^{-1}$  ( $5.56 \times 10^{-7} \text{ s}^{-1}$ ) in the summer on a sunny day in the Gulf of Mexico. Using a summertime surface seawater dissolved acrylate concentration of 1.5 nM in the Gulf of Mexico,<sup>30</sup> the corresponding potential maximum primary photolysis rate of acrylate at the sea surface is  $0.003 \text{ nM h}^{-1}$ . When the concentration of acrylate is low as observed in the Gulf of Mexico, the maximum rate of primary photolysis at the sea surface is quite slow, approximately an order of magnitude or more slower than photochemical production rates of acrylate ( $0.034$  to  $0.14 \text{ nM h}^{-1}$ ).

Secondary photolysis of acrylate through the reaction with ROS should also be insignificant because ambient seawater concentrations of both acrylate and ROS are too low. For example, 1.5 nM acrylate<sup>30</sup> reacts with  $2 \times 10^{-18} \text{ M}$  hydroxyl radical<sup>58</sup> with a diffusion-controlled second-order rate constant of  $1.9 \times 10^{10} \text{ M}^{-1} \text{ s}^{-1}$ .<sup>59</sup> The resultant loss rate is  $2 \times 10^{-13} \text{ M h}^{-1}$  corresponding to a turnover time of 2 years.

Even though theoretical calculations suggest that acrylate should not photolyze in seawater at ambient acrylate concentrations, published results have shown that acrylate photolyzes in both pure water and seawater at  $\mu\text{M}$  concentrations.<sup>31,32</sup> Reported rate constants for the photolysis

of acrylate in seawater exposed to sunlight,  $1.3 \times 10^{-7,31}$  and  $3.0 \times 10^{-6} \text{ s}^{-1,32}$  are slow, significantly less than the maximum theoretical rate constant that we calculated for the primary photolysis of acrylate in the summer in the Gulf of Mexico. This suggests that acrylate photolysis should be slow in seawater at ambient nM concentrations.

We tested this assumption by exposing a 20.1 or 100 nM DMSP-derived acrylate standard (or sodium acrylate-derived acrylate standard) in Milli-Q water (circumneutral pH) or seawater to the solar simulator for up to 12 h. We observed no acrylate photolysis in Milli-Q water (Figure 5D; Figure S6A). Likewise, no photolysis was seen when sodium acrylate was used as the acrylate source for the photolysis experiment. Acrylate was photochemically produced in seawater from coastal Rhode Island (ca. 6 nM) and the Sargasso Sea (ca. 2 nM) amended with 100 nM acrylate (Figure S6A). The same rate of increase was observed in the 20.1 nM acrylate amended samples (data not shown) and in unamended coastal Rhode Island and Sargasso Sea samples (Figure 3). Since acrylate production was the same in all coastal Rhode Island or Sargasso Sea samples, irrespective of the initial acrylate concentration (0.5, 20.1, or 100 nM), this indicates that photolysis was not important. For comparison, the predicted photolysis rate of 100 nM acrylate in seawater was plotted using published rate constants<sup>31,32</sup> after scaling rates to the photon exposure in our solar simulator (Figure S6B).

Since photolysis was not observed in Milli-Q water (Figure 5D) and since photochemical production rates with and without added acrylate were not significantly different ( $t$  test,  $p > 0.05$ ), then it must be concluded that acrylate does not photolyze in seawater, at least for acrylate concentrations  $> 100 \text{ nM}$ . We postulate that photolysis did not occur at low nM concentrations because the triplet excited state, corresponding to the n-to- $\pi^*$  transition,<sup>56</sup> rapidly relaxed and returned to the ground state by either triplet energy transfer to DOM or dissolved oxygen or collisional deactivation by water.<sup>56</sup>

There are several reasons why our results likely differed from previous studies.<sup>31,32</sup> First, we conducted photolysis experiments using nM acrylate concentrations, significantly lower than the  $\mu\text{M}$  levels used in previous studies.<sup>31,32</sup> Acrylate concentrations in the low to high  $\mu\text{M}$  range would favor reactions between acrylate and ROS that are not important for acrylate photolysis at low nM levels, as previously discussed for the hydroxyl radical – acrylate reaction. Another potential issue with prior studies is that photosensitized reactions between two acrylate molecules or between acrylate and the stabilizer (e.g., 4-methoxyphenol, used to stabilize acrylic acid) may have occurred at  $\mu\text{M}$  acrylate concentrations. Acrylate–acrylate reactions are not expected to be important at low nM concentrations, and potential stabilizer reactions are avoided when using DMSP-derived acrylate in photolysis experiments, as was done in our study. An added complication in the Wu et al. study is that they added sodium azide as a biological poison prior to sample filtration.<sup>32</sup> They observed that acrylate ( $260 \pm 182$  nM,  $n = 8$ ) rapidly photolyzed in Jiaozhou Bay waters when exposed to sunlight with an average ( $\pm$ std. dev) first-order rate constant of  $5.5 \pm 4.3$  day<sup>-1</sup> ( $n = 8$ ).<sup>32</sup> This rapid photolysis was not interpreted by the authors, but it may have resulted from the use of sodium azide resulting in release of organic matter from microorganisms.

**Implications for Marine Acrylate Cycling.** The photochemical production of acrylate represents a new source for this compound in seawater with production rates ranging from 0.34 to 1.44 nM day<sup>-1</sup> in our study, assuming 10 h of solar radiation. These daily rates fall within the lower end of the range of estimated rates for its production from the enzymatic cleavage of DMSP by lyase based on published DMS production rates of <0.1 to 7.7 nM day<sup>-1</sup> (refs 18–26), suggesting that photochemical production is a quantitatively important production pathway for acrylate in seawater. Our photochemical production rates are similar to or by a factor of 2 faster than the biological consumption rate of acrylate in Gulf of Mexico coastal (1.16 vs 0.96 nM day<sup>-1</sup>) or open ocean (0.48 vs 0.24 nM day<sup>-1</sup>) waters, respectively, suggesting that photochemical production may be sufficiently fast to support acrylate's role as a carbon and energy source for the growth of selected heterotrophs in the Gulf of Mexico.

Direct release of acrylate from phytoplankton should also contribute to the dissolved pool of acrylate. In axenic *P. antarctica* cultures, a large fraction of the total acrylate (up to 95%) was present in the dissolved phase.<sup>6</sup> The authors suggested that the high dissolved acrylate concentrations may have resulted from either its intracellular production and subsequent e ux from the cell or its production from extracellular lysis of DMSP. Although significant release was noted in culture, rates of algal production of dissolved acrylate in the oceans are not known and warrant further investigation to assess the relative importance of this biological source relative to photoproduction of acrylate in seawater.

## ■ ASSOCIATED CONTENT

### SI Supporting Information

The Supporting Information is available free of charge at <https://pubs.acs.org/doi/10.1021/acs.est.1c00327>.

Calculation of hourly based clear sky photochemical production rates of acrylate in seawater (Section S1), sampling locations (Figure S1), the spectral irradiance output of the 300 W xenon lamp (Figure S2), nitrite-

based photochemical production rates of acrylate plotted against the CDOM absorption coefficient at 290 or 390 nm (Figure S3), the decrease of CDOM absorption coefficients during the solar-simulator irradiation of seawater (Figure S4), sunlight photochemical production rates plotted against corresponding scaled solar-simulator rates (Figure S5), the photochemical production of acrylate in seawater at an initial acrylate concentration of 100 nM and the predicted loss of acrylate using rate constants reported in previous studies (Figure S6), and hourly photoproduction rates under clear-sky conditions and the data used to calculate these rates (Table S1) (PDF)

## ■ AUTHOR INFORMATION

### Corresponding Author

David J. Kieber – Department of Chemistry, State University of New York, College of Environmental Science and Forestry, Syracuse, New York 13210, United States; [orcid.org/0000-0001-6532-950X](https://orcid.org/0000-0001-6532-950X); Phone: 1-315-470-6951; Email: [djkieber@esf.edu](mailto:djkieber@esf.edu); Fax: 1-315-470-6856

### Author

Lei Xue – Department of Chemistry, State University of New York, College of Environmental Science and Forestry, Syracuse, New York 13210, United States; [orcid.org/0000-0002-5343-8079](https://orcid.org/0000-0002-5343-8079)

Complete contact information is available at: <https://pubs.acs.org/10.1021/acs.est.1c00327>

### Notes

The authors declare no competing financial interest.

## ■ ACKNOWLEDGMENTS

The authors thank the National Science Foundation Chemical Oceanography program for financial support (CO-1756907, D.J.K.). Thanks are also extended to Dr. Rafel Simó and his research team, who assisted with seawater collection during the fieldwork in the Mo'orea coral reef and the Pacific Ocean, the UC Berkeley South Pacific Research Station for their logistical support, and Dr. Cèlia Marrasé for lending her fluorometer to us for actinometry measurements during the Mo'orea field study.

## ■ REFERENCES

- (1) Keller, M. D.; Bellows, W. K.; Guillard, R. R. L. Dimethyl sulfide production in marine phytoplankton. In *Biogenic Sulfur in the Environment*; Saltzman, E. S.; Cooper, W. J., Eds.; ACS Symp. Ser.: 1989, 393, pp. 167–182.
- (2) Keller, M. D.; Kiene, R. P.; Matrai, P. A.; Bellows, W. K. Production of glycine betaine and dimethylsulfoniopropionate in marine phytoplankton. I. Batch cultures. *Mar. Biol.* **1999**, *135*, 237–248.
- (3) Raina, J.-B.; Tapiolas, D. M.; Forêt, S.; Lutz, A.; Abrego, D.; Ceh, J.; Seneca, F. O.; Clode, P. L.; Bourne, D. G.; Willis, B. L.; Motti, C. A. DMSP biosynthesis by an animal and its role in coral thermal stress response. *Nature* **2013**, *502*, 677–680.
- (4) Curson, A. R. J.; Liu, J.; Martínez, A. B.; Green, R. T.; Chan, Y.; Carrión, O.; Williams, B. T.; Zhang, S.-H.; Yang, G.-P.; Page, P. C. B.; Zhang, X.-H.; Todd, J. D. Dimethylsulfoniopropionate biosynthesis in marine bacteria and identification of the key gene in this process. *Nat. Microbiol.* **2017**, *2*, 17009.
- (5) Williams, B. T.; Cowles, K.; Martínez, A. B.; Curson, A. R. J.; Zheng, Y.; Liu, J.; Newton-Payne, S.; Hind, A. J.; Li, C.-Y.; Rivera, P.

- P. L.; Carrión, O.; Liu, J.; Spurgin, L. G.; Brearley, C. A.; Mackenzie, B. W.; Pinchbeck, B. J.; Peng, M.; Pratscher, J.; Zhang, X.-H.; Zhang, Y.-Z.; Murrell, J. C.; Todd, J. D. Bacteria are important dimethylsulfoniopropionate producers in coastal sediments. *Nat. Microbiol.* **2019**, *4*, 1815–1825.
- (6) Kinsey, J. D.; Kieber, D. J.; Neale, P. J. Effects of iron limitation and UV radiation on *Phaeocystis antarctica* growth and DMSP, DMSO, and acrylate concentrations. *Environ. Chem.* **2016**, *13*, 195–211.
- (7) Yang, H.; McTaggart, A. R.; Davidson, A. T.; Burton, H. Measurement of acrylic acid and dimethylsulfide in Antarctic coastal water during a summer bloom of *Phaeocystis pouchetii*. *Proc. NIPR Symp. Polar Biol.* **1994**, *7*, 43–52.
- (8) Gibson, J. A. E.; Swadling, K. M.; Burton, H. R. Acrylate and Dimethylsulfoniopropionate (DMSP) concentrations during an Antarctic phytoplankton bloom. In *Biological and Environmental Chemistry of DMSP and Related Sulfonium Compounds*; Kiene, R. P.; Visscher, P. T.; Keller, M. D.; Kirst, G. O., Eds.; Plenum Press: New York 1996; pp. 213–222.
- (9) Sunda, W.; Kieber, D. J.; Kiene, R. P.; Huntsman, S. An antioxidant function for DMSP and DMS in marine algae. *Nature* **2002**, *418*, 317–320.
- (10) Stefels, J. Physiological aspects of the production and conversion of DMSP in marine algae and higher plants. *J. Sea Res.* **2000**, *43*, 183–197.
- (11) Sieburth, J. M. Acrylic acid, an “antibiotic” principle in *Phaeocystis* blooms in Antarctic waters. *Science* **1960**, *132*, 676–677.
- (12) Slezak, D. M.; Puskaric, S.; Herndl, G. J. Potential role of acrylic acid in bacterioplankton communities in the sea. *Mar. Ecol. Prog. Ser.* **1994**, *105*, 191–197.
- (13) Wolfe, G. V.; Steinke, M.; Kirst, G. O. Grazing-activated chemical defence in a unicellular marine alga. *Nature* **1997**, *387*, 894–897.
- (14) van Alstyne, K. L.; Wolfe, G. V.; Freidenburg, T. L.; Neill, A.; Hicken, C. Activated defense systems in marine macroalgae: evidence for an ecological role for DMSP cleavage. *Mar. Ecol. Prog. Ser.* **2001**, *213*, 53–65.
- (15) Evans, C.; Kadner, S. V.; Darroch, L. J.; Wilson, W. H.; Liss, P. S.; Malin, G. The relative significance of viral lysis and microzooplankton grazing as pathways of dimethylsulfoniopropionate (DMSP) cleavage: An *Emiliania huxleyi* culture study. *Limnol. Oceanogr.* **2007**, *52*, 1036–1045.
- (16) Noordkamp, D. J. B.; Gieskes, W. W. C.; Gottschal, J. C.; Forney, L. J.; van Rijssel, M. Acrylate in *Phaeocystis* colonies does not affect the surrounding bacteria. *J. Sea Res.* **2000**, *43*, 287–296.
- (17) Dacey, J. W. H.; Blough, N. V. Hydroxide decomposition of DMSP to form DMS. *Geophys. Res. Lett.* **1987**, *14*, 1246–1249.
- (18) Kiene, R. P.; Linn, L. J. Distribution and turnover of dissolved DMSP and its relationship with bacterial production and dimethylsulfide in the Gulf of Mexico. *Limnol. Oceanogr.* **2000**, *45*, 849–861.
- (19) Zubkov, M. V.; Fuchs, B. M.; Archer, S. D.; Kiene, R. P.; Amann, R.; Burkill, P. H. Rapid turnover of dissolved DMS and DMSP by defined bacterioplankton communities in the stratified euphotic zone of the North Sea. *Deep Sea Res., Part II* **2002**, *49*, 3017–3038.
- (20) Merzouk, A.; Levasseur, M.; Scarratt, M.; Michaud, S.; Lizotte, M.; Rivkin, R. B.; Kiene, R. P. Bacterial DMSP metabolism during the senescence of the spring diatom bloom in the Northwest Atlantic. *Mar. Ecol. Prog. Ser.* **2008**, *369*, 1–11.
- (21) Vila-Costa, M.; Kiene, R. P.; Simó, R. Seasonal variability of the dynamics of dimethylated sulfur compounds in a coastal northwest Mediterranean site. *Limnol. Oceanogr.* **2008**, *53*, 198–211.
- (22) Royer, S.-J.; Levasseur, M.; Lizotte, M.; Arychuk, M.; Scarratt, M. G.; Wong, C. S.; Lovejoy, C.; Robert, M.; Johnson, K.; Peña, A.; Michaud, S.; Kiene, R. P. Microbial dimethylsulfoniopropionate (DMSP) dynamics along a natural iron gradient in the northeast subarctic Pacific. *Limnol. Oceanogr.* **2010**, *55*, 1614–1626.
- (23) Luce, M.; Levasseur, M.; Scarratt, M. G.; Michaud, S.; Royer, S.-J.; Kiene, R. P.; Lovejoy, C.; Gosselin, M.; Poulin, M.; Gratton, Y.; Lizotte, M. Distribution and microbial metabolism of dimethylsulfoniopropionate and dimethylsulfide during the 2007 Arctic ice minimum. *J. Geophys. Res.* **2011**, *116*, C00G06.
- (24) Motard-Côté, J.; Kieber, D. J.; Rellinger, A.; Kiene, R. P. Influence of the Mississippi River plume and nonbioavailable DMSP on dissolved DMSP turnover in the northern Gulf of Mexico. *Environ. Chem.* **2016**, *13*, 280–292.
- (25) Lizotte, M.; Levasseur, M.; Michaud, S.; Scarratt, M. G.; Merzouk, A.; Gosselin, M.; Pommier, J.; Rivkin, R. B.; Kiene, R. P. Macroscale patterns of the biological cycling of dimethylsulfoniopropionate (DMSP) and dimethylsulfide (DMS) in the Northwest Atlantic. *Biogeochemistry* **2012**, *110*, 183–200.
- (26) Lizotte, M.; Levasseur, M.; Law, C. S.; Walker, C. F.; Safi, K. A.; Marriner, A.; Kiene, R. P. Dimethylsulfoniopropionate (DMSP) and dimethyl sulfide (DMS) cycling across contrasting biological hotspots of the New Zealand subtropical front. *Ocean Sci.* **2017**, *13*, 961–982.
- (27) Ledyard, K. M.; DeLong, E. F.; Dacey, J. W. H. Characterization of a DMSP-degrading bacterial isolate from the Sargasso Sea. *Arch. Microbiol.* **1993**, *160*, 312–318.
- (28) González, J. M.; Kiene, R. P.; Moran, M. A. Transformation of sulfur compounds by an abundant lineage of marine bacteria in the - subclass of the class *Proteobacteria*. *Appl. Environ. Microbiol.* **1999**, *65*, 3810–3819.
- (29) Garren, M.; Son, K.; Raina, J.-B.; Rusconi, R.; Menolascina, F.; Shapiro, O. H.; Tout, J.; Bourne, D. G.; Seymour, J. R.; Stocker, R. A bacterial pathogen uses dimethylsulfoniopropionate as a cue to target heat-stressed corals. *ISME J.* **2014**, *8*, 999–1007.
- (30) Tyssebotn, I. M. B.; Kinsey, J. D.; Kieber, D. J.; Kiene, R. P.; Rellinger, A. N.; Motard-Côté, J. Concentrations, biological uptake, and respiration of dissolved acrylate and dimethylsulfoxide in the northern Gulf of Mexico. *Limnol. Oceanogr.* **2017**, *62*, 1198–1218.
- (31) Bajt, O.; Šket, B.; Faganeli, J. The aqueous photochemical transformation of acrylic acid. *Mar. Chem.* **1997**, *58*, 255–259.
- (32) Wu, X.; Liu, C.-Y.; Li, P.-F. Photochemical transformation of acrylic acid in seawater. *Mar. Chem.* **2015**, *170*, 29–36.
- (33) Vairavamurthy, A.; Andreae, M. O.; Brooks, J. M. Determination of acrylic acid in aqueous samples by electron capture gas chromatography after extraction with tri-*n*-octylphosphine oxide and derivatization with pentafluorobenzyl bromide. *Anal. Chem.* **1986**, *58*, 2684–2687.
- (34) Kieber, D. J.; Yocis, B. H.; Mopper, K. Free-floating drifter for photochemical studies in the water column. *Limnol. Oceanogr.* **1997**, *42*, 1829–1833.
- (35) Xue, L. Acrylate: The missing carbon in the marine organosulfur cycle. Ph.D. Dissertation, State University of New York, College of Environmental Science and Forestry: Syracuse, NY, 2020.
- (36) Toole, D. A.; Kieber, D. J.; Kiene, R. P.; Siegel, D. A.; Nelson, N. B. Photolysis and the dimethylsulfide (DMS) summer paradox in the Sargasso Sea. *Limnol. Oceanogr.* **2003**, *48*, 1088–1100.
- (37) Jankowski, J. J.; Kieber, D. J.; Mopper, K. Nitrate and nitrite ultraviolet actinometers. *Photochem. Photobiol.* **1999**, *70*, 319–328.
- (38) Jankowski, J. J.; Kieber, D. J.; Mopper, K.; Neale, P. J. Development and intercalibration of ultraviolet solar actinometers. *Photochem. Photobiol.* **2000**, *71*, 431–440.
- (39) Kieber, D. J.; Toole, D. A.; Jankowski, J. J.; Kiene, R. P.; Westby, G. R.; del Valle, D. A.; Slezak, D. Chemical “light meters” for photochemical and photobiological studies. *Aquat. Sci.* **2007**, *69*, 360–376.
- (40) Kinsey, J. D.; Kieber, D. J. Microwave preservation method for DMSP, DMSO, and acrylate in unfiltered seawater and phytoplankton culture samples. *Limnol. Oceanogr.: Methods* **2016**, *14*, 196–209.
- (41) Kieber, D. J.; Miller, G. W.; Neale, P. J.; Mopper, K. Wavelength and temperature-dependent apparent quantum yields for photochemical formation of hydrogen peroxide in seawater. *Environ. Sci.: Process. Impacts* **2014**, *16*, 777–791.

(42) Cartisano, C. M.; Del Vecchio, R.; Blough, N. V. A calibration/validation protocol for long/multi-pathlength capillary waveguide spectrometers. *Limnol. Oceanogr.: Methods* **2018**, *16*, 773–786.

(43) Kieber, R. J.; Zhou, X.; Mopper, K. Formation of carbonyl compounds from UV-induced photodegradation of humic substances in natural waters: Fate of riverine carbon in the sea. *Limnol. Oceanogr.* **1990**, *35*, 1503–1515.

(44) de Bruyn, W. J.; Clark, C. D.; Pagel, L.; Takehara, C. Photochemical production of formaldehyde, acetaldehyde and acetone from chromophoric dissolved organic matter in coastal waters. *J. Photochem. Photobiol., A* **2011**, *226*, 16–22.

(45) Stubbins, A.; Law, C. S.; Uher, G.; Upstill-Goddard, R. C. Carbon monoxide apparent quantum yields and photoproduction in the Tyne estuary. *Biogeosciences* **2011**, *8*, 703–713.

(46) Zhu, Y.; Kieber, D. J. Global model for depth-dependent carbonyl photochemical production rates in seawater. *Global Biogeochem. Cycles* **2020**, *34*, No. e2019GB006431.

(47) Mopper, K.; Zhou, X.; Kieber, R. J.; Kieber, D. J.; Sikorski, R. J.; Jones, R. D. Photochemical degradation of dissolved organic carbon and its impact on the oceanic carbon cycle. *Nature* **1991**, *353*, 60–62.

(48) White, E. M.; Kieber, D. J.; Sherrard, J.; Miller, W. L.; Mopper, K. Carbon dioxide and carbon monoxide photoproduction quantum yields in the Delaware Estuary. *Mar. Chem.* **2010**, *118*, 11–21.

(49) Zhu, Y.; Kieber, D. J. Concentrations and photochemistry of acetaldehyde, glyoxal, and methylglyoxal in the Northwest Atlantic Ocean. *Environ. Sci. Technol.* **2019**, *53*, 9512–9521.

(50) Mopper, K.; Stahovec, W. L. Sources and sinks of low molecular weight organic carbonyl compounds in seawater. *Mar. Chem.* **1986**, *19*, 305–321.

(51) Zhou, X.; Mopper, K. Photochemical production of low-molecular-weight carbonyl compounds in seawater and surface microlayer and their air-sea exchange. *Mar. Chem.* **1997**, *56*, 201–213.

(52) Takeda, K.; Katoh, S.; Mitsui, Y.; Nakano, S.; Nakatani, N.; Sakugawa, H. Spatial distributions of and diurnal variations in low molecular weight carbonyl compounds in coastal seawater, and the controlling factors. *Sci. Total Environ.* **2014**, *493*, 454–462.

(53) Zhu, Y.; Kieber, D. J. Wavelength and temperature-dependent apparent quantum yields for photochemical production of carbonyl compounds in the North Pacific Ocean. *Environ. Sci. Technol.* **2018**, *52*, 1929–1939.

(54) Bouillon, R.-C.; Knierim, T. L.; Kieber, R. J.; Skrabal, S. A.; Wright, J. L. C. Photodegradation of the algal toxin domoic acid in natural water matrices. *Limnol. Oceanogr.* **2006**, *51*, 321–330.

(55) Yocis, B. H.; Kieber, D. J.; Mopper, K. Photochemical production of hydrogen peroxide in Antarctic Waters. *Deep-Sea Res., Part I* **2000**, *47*, 1077–1099.

(56) Rosenfeld, R. N.; Weiner, B. R. Photofragmentation of acrylic acid and methacrylic acid in the gas phase. *J. Am. Chem. Soc.* **1983**, *105*, 6233–6236.

(57) Leifer, A. *The Kinetics of Environmental Aquatic Photochemistry: Theory and Practice*; American Chemical Society: Washington, DC, 1988.

(58) Zhou, X.; Mopper, K. Determination of photochemically produced hydroxyl radicals in seawater and freshwater. *Mar. Chem.* **1990**, *30*, 71–88.

(59) Buxton, G. V.; Greenstock, C. L.; Helman, W. P.; Ross, A. B. Critical review of rate constants for reactions of hydrated electrons, hydrogen atoms and hydroxyl radicals in aqueous solution ( $\cdot\text{OH}/\cdot\text{O}^-$ ) in aqueous solution. *J. Phys. Chem. Ref. Data* **1988**, *17*, 513–886.